infrastructures

MDPI

Article

Cradle-to-Gate Life Cycle and Economic Assessment of Sustainable Concrete Mixes—Alkali-Activated Concrete (AAC) and Bacterial Concrete (BC)

Kruthi Kiran Ramagiri [1,*], Ravali Chintha [1], Radha Kiranmaye Bandlamudi [1], Patricia Kara De Maeijer [2] and Arkamitra Kar [1]

[1] Department of Civil Engineering, Birla Institute of Technology and Science-Pilani, Hyderabad Campus, Hyderabad 500078, Telangana, India; h20191430099@hyderabad.bits-pilani.ac.in (R.C.); p20180462@hyderabad.bits-pilani.ac.in (R.K.B.); arkamitra.kar@hyderabad.bits-pilani.ac.in (A.K.)

[2] EMIB, Faculty of Applied Engineering, University of Antwerp, Groenenborgerlaan 171, 2020 Antwerp, Belgium; patricija.karademaeijer@uantwerpen.be

* Correspondence: p20170008@hyderabad.bits-pilani.ac.in

Abstract: The negative environmental impacts associated with the usage of Portland cement (PC) in concrete induced intensive research into finding sustainable alternative concrete mixes to obtain "green concrete". Since the principal aim of developing such mixes is to reduce the environmental impact, it is imperative to conduct a comprehensive life cycle assessment (LCA). This paper examines three different types of sustainable concrete mixes, viz., alkali-activated concrete (AAC) with natural coarse aggregates, AAC with recycled coarse aggregates (RCA), and bacterial concrete (BC). A detailed environmental impact assessment of AAC with natural coarse aggregates, AAC with RCA, and BC is performed through a cradle-to-gate LCA using openLCA v.1.10.3 and compared versus PC concrete (PCC) of equivalent strength. The results show that transportation and sodium silicate in AAC mixes and PC in BC mixes contribute the most to the environmental impact. The global warming potential (GWP) of PCC is 1.4–2 times higher than other mixes. Bacterial concrete without nutrients had the lowest environmental impact of all the evaluated mixes on all damage categories, both at the midpoint (except GWP) and endpoint assessment levels. AAC and BC mixes are more expensive than PCC by 98.8–159.1% and 21.8–54.3%, respectively.

Keywords: life cycle assessment (LCA); bacterial concrete (BC); environmental impact assessment; alkali-activated concrete (AAC); alkali-activated binder (AAB); recycled coarse aggregates

Citation: Ramagiri, K.K.; Chintha, R.; Bandlamudi, R.K.; Kara De Maeijer, P.; Kar, A. Cradle-to-Gate Life Cycle and Economic Assessment of Sustainable Concrete Mixes— Alkali-Activated Concrete (AAC) and Bacterial Concrete (BC). *Infrastructures* **2021**, *6*, 104. https://doi.org/10.3390/infrastructures6070104

Academic Editor: Ali Behnood

Received: 28 June 2021
Accepted: 13 July 2021
Published: 15 July 2021

1. Introduction

To mitigate the worst health impacts of climate change, global annual greenhouse gas (GHG) emissions must be halved by 2030 and attain net-zero by 2050 [1] or incur the marginal expense of negative emissions. This expense could be in the range of USD 100–300/t CO_2-Eq. depending on the cost of biomass or direct CO_2 capture through carbon capture and storage [2]. The global energy-associated CO_2 emissions from the building sector alone accounted for 38% of the total emissions in 2019 [3]. The Paris Agreement, an international legal treaty adopted by 196 states, aims to limit global warming to 1.5 °C compared to pre-industrial levels [4]. The International Energy Agency (IEA) estimates that to achieve net-zero emissions by 2050, the direct and indirect CO_2 emissions from the building sector should decline by 50% and 60%, respectively, by 2030 [3]. Portland cement (PC) is the primary contributor of emissions in the building sector, accounting for approximately 14% of non-energy use CO_2 emissions, owing to its significant use and innate characteristics of its manufacturing process [5]. Energy conservation, carbon extraction, and the use of alternative materials are some of the strategies for reducing CO_2 pollution associated with the use of PC, which were lately introduced [6].

Recent research reports the use of materials such as calcined clay, marble dust, and granite dust as PC replacements for improving the sustainability of concrete production [7,8]. Utilizing industrial wastes, bio-wastes, and agro-wastes with alternative activations such as alkali-activation and carbonation has been performed in various applications [9–11]. Alkali-activated binders (AABs) have shown significant potential in replacing PC in concrete mixes [12–14]. AAB concrete, viz., alkali-activated concrete (AAC), produced by the activation of aluminosilicate-rich industrial wastes with an alkaline activator, exhibits superior mechanical and durability performance and a lower carbon footprint than PC concrete (PCC) [15]. The commonly used precursors in AAC are fly ash and ground granulated blast furnace slag (GGBFS, further referred to as slag). There is extensive literature available on fly ash-based AAC compared to slag-based AAC [16]. Furthermore, previous research shows that slag can be effectively used as a precursor when used in combination with other alternative binders such as fly ash or glass powder [11]. However, the latest tendency of the application of alternative binders has to also be investigated in depth in regard to the environmental impact.

In addition to the emissions associated with binders used in concrete, the use of natural aggregates (NA) (usually limestone or granite) results in resource scarcity, deterring its sustainable development. NA can be replaced with recycled aggregates, resulting in the twofold advantage of minimizing the extraction of non-renewable sources and environmental impact from disposed of resources. Construction and demolition waste (CDW) generated in India is estimated to be about 100 million tonnes yearly. The utilization of CDW in India constitutes only 10–30% of the generation. In the European Union (EU), for example, 850 million tonnes are generated per year and 70% are set to be recycled by 2020 according to the Waste Framework Directive [17]. Usually, CDW is primarily used for land-leveling and backfilling projects, while the remaining is disposed of in landfills [18]. CDW from building-derived materials (BDM) can be a potential partial replacement of NA in PC and AAC [19,20]. The effect of incorporating recycled coarse aggregates (RCA) on the mechanical properties and durability of PCC has been extensively reported in the literature [21–23]. The lower replacement levels of about 20% of NA with RCA did not alter the mechanical performance of PCC [22]. However, a further increase in the replacement percentage reduced the mechanical strength. This reduction in strength is attributed to increased porosity and a weak interfacial transition zone (ITZ) between aggregates and the matrix [24]. AAB concrete exhibited a higher potential for the replacement of NA with RCA. The change in compressive strength is reported in the range of 20% when 50% of NA is replaced with RCA [25]. Due to the increased porosity, the addition of RA has a negative impact on the durability of PCC. However, because of the higher alkaline environment of the alkali-activated systems, recycled aggregates could be more suitable for use [25]. It is evident from the existing literature that alternative binders and RCA could be used as a complete or partial substitute for their conventional counterparts.

However, the main rationale for their use is to improve sustainable development, which necessitates a rigorous environmental assessment to determine their efficacy. A few studies reported that replacing PCC with AAC can reduce the emissions associated with climate change by 9–80% compared to PCC [26,27]. This significant disparity in emissions' mitigation by AAC is due to differences in the types of precursors and activators, mix proportions, transit distances, and the type of production and sources of raw materials. There have been relatively few investigations on the environmental effects of RCA inclusion in AAC. The treatment procedures used to improve the quality of RCA can result in additional environmental burdens. Since the adhered matrix is the phase increasing porosity, treatment approaches are commonly used to extract it from the surface of RCA. The treatment approaches include either dissolving RCA in a solvent or imposing internal tension at their ITZ to isolate them from the adhered hardened binder. The treatment processes used in previous studies on AAC are ultrasonic cleaning [28], pre-saturation [29], carbon dioxide sequestration (CS) [30], nitric acid dissolution [29], thermal expansion [31], the freeze–thaw method [32], microwave heating [33], mechanical grinding [34], and the

heating and rubbing method [35]. Most of the above-mentioned treatment processes are energy and/or resource-intensive. Using RCA treated through CS improved the compressive strength by approximately nine times due to more stable polymorphs. Furthermore, CS-treated RCA can reduce GHG emissions by 50% compared to NA cured under ambient conditions [30]; however, they increased the cost/m^3 of concrete owing to the higher cost of RCA. Furthermore, to promote in situ applications of AAC with RCA, a detailed environmental analysis is necessary. As a preliminary step, the present study aims to evaluate the environmental and economic impact of untreated (virgin) BDM used as coarse aggregates in AAC.

The other aspect of concrete structures that can incur high cost is their repair and maintenance. The proclivity of concrete for cracking is the primary factor compromising its structural integrity, serviceability, and durability. Conventional rehabilitation and maintenance are effective strategies for prolonging the service life of concrete structures. However, the repair and maintenance cost of concrete cracking can be 84% to 125% higher than the actual construction cost/m^3 [36]. The USA spends USD 266.5 billion on infrastructure maintenance and repair, accounting for 65% of all public infrastructure expenditures [37]. Infrastructure assessment, repair, and maintenance account for nearly 33% and 45% of the annual civil engineering budgets in The Netherlands and the United Kingdom, respectively [38,39]. According to recent estimates, India spends about 1.08% of its annual GDP on infrastructure repair and maintenance [40]. Furthermore, depending on the location of the crack, its extent, and the service needs for infrastructures such as highways, there might be situations where repair is impractical. Self-healing concrete can be very beneficial in these circumstances by automatically healing fractures without the need for external intervention [41].

Self-healing can be achieved through two different mechanisms, viz., autogenous and autonomous healing. Autogenous healing refers to reactions and/or processes originating from the cementitious system, such as calcium hydroxide carbonation, crack blockage caused by impurities in water and loose concrete particles, and ongoing hydration of cement [42], whereas autonomous healing comprises the utilization of additions/methods such as bacteria, shape memory alloy capsules, and electrodeposition technology. Autonomous healing via the addition of mineral-depositing bacteria is one of the most efficient and potentially sustainable methodologies [43].

The bacteria added along with the nutrients to the concrete mix is activated when it encounters the moisture through the newly formed cracks and begins the precipitation of calcium carbonate through metabolism. There are three major metabolic pathways to precipitate calcium carbonate, viz., the hydrolysis of urea, the oxidation of organic compounds, and denitrification depending on the type of bacteria [43–45]. Different ureolytic bacteria such as *Sporosarcina ureae*, *Bacillus sphaericus*, *Bacillus megaterium*, *Proteus vulgaris*, *Proteus mirabilis*, *Bacillus subtilis*, and *Sporosarcina pasteurii* have been used in self-healing concrete [46]. Denitrifying bacteria such as *Pseudomonas aeruginosa* and *Diaphorobacter nitroreducens* and aerobic heterotrophic bacteria (which produces calcium carbonate by the oxidation of organic compounds) such as *Bacillus pseudoformus* and *Bacillus cohnii* are also used in successfully developing self-healing behavior in concrete [45,46].

Bacterial concrete is reported to enhance compressive strength by approximately 40% under simulated cracks by healing them [47]. There is an optimum concentration of bacteria that shows a positive effect on the compressive strength of bacterial concrete with fly ash, and it is reported to be 10^5 cells/mL for *Sporoscarcina pasteurii* bacteria [48]. Studies show that the direct inclusion of bacteria, that is, without immobilization or encapsulation, improved compressive strength in the range of 15–32% [49,50], flexural strength by 11% [49], and split tensile strength by 14–16% [49,50]. The immobilization and encapsulation of bacteria are known to improve the self-healing efficiency of concrete [51]. Limestone powder [52], iron oxide nano-sized particles [53], crushed brick aggregate [54], graphite nanoplatelets [55], expanded perlite [56], and porous ceramsite particles [57] are used for the immobilization of bacteria in concrete. Though efficient, the shortcoming of

protective materials is their varying efficiencies depending on the type. Encapsulation resulted in a healing rate of 70 to 100% for cracks in the range of 0.3 mm [58]. Typically used Ca-precursors for aerobic respiration in bacterial concrete are calcium acetate, calcium lactate, calcium nitrate, and calcium formate [59]. Calcium nitrate acts as an accelerator when added to concrete, reducing the setting times, accelerating hydration, and decreasing compressive strength [59,60]. It is reported that calcium lactate used in the range of 1–2% by mass of cement improved its compressive strength; however, there are contradictory studies on its effect on setting times [59,61]. Calcium formate and calcium acetate are also found to be suitable Ca-precursors based on compressive strength investigations [59]. It is evident that there is extensive literature reported on the mechanical performance of bacterial concrete. However, to the best of the authors' knowledge, there are no studies on the environmental assessment of bacterial concrete.

The present study performs a comprehensive life cycle assessment of three different sustainable concrete mixes: alkali-activated concrete (AAC) with natural coarse aggregates, (2) AAC with recycled coarse aggregates, and bacterial concrete (BC) with and without Ca-precursors. AAC with natural coarse aggregates, AAC with RCA, and BC are evaluated using a cradle-to-gate life cycle assessment (LCA) and compared to PCC of equal strength. The influence of mix proportions on the environmental impact of three distinct AAC mixes and two distinct BC mixes is investigated. The life cycle impact assessment is performed both at midpoint and endpoint damage categories using ReCiPe 2016 methodology. Simple cost analysis, including electricity, water tariffs and transportation charges in the Indian context, is presented.

2. Materials and Methods

2.1. Materials

The precursors considered in the present study are class F fly ash, slag, and Portland cement (PC). Class F fly ash utilized in this investigation is obtained from the National Thermal Power Corporation in Ramagundam, India. Slag is acquired from JSW Ltd. in Vijayanagar, India. In the current investigation, Type I Portland cement of 53 grade complying to the standards IS [62] and ASTM [63] requirements is used. The properties of the precursors are provided in Table 1.

Table 1. Specifications of precursors.

Specification	Fly Ash	Slag	PC
CaO (%)	3.80	37.63	65.23
SiO_2 (%)	48.81	34.81	18.64
Al_2O_3 (%)	31.40	17.92	5.72
MgO (%)	0.70	7.80	0.85
SO_3 (%)	0.91	0.20	2.34
Fe_2O_3 (%)	7.85	0.66	4.54
TiO_2 (%)	2.93	-	0.5
K_2O (%)	1.52	-	0.59
Na_2O (%)	1.04	-	-
MnO (%)	-	0.21	-
LOI (%)	3.00	1.41	1.69
Strength activity index (%)	96.46	114.46	-
d_{50} (µm)	51.90	13.93	-
Blaine fineness (m^2/kg) *	327.00	386.00	285.00
Specific gravity	2.06	2.71	-

* Supplied by manufacturer.

Locally available river sand and crushed rock fines (CRF) are used as fine aggregates in the present study. Crushed granite with a nominal maximum size of 10 mm is used as coarse aggregate. River sand and crushed granite aggregates comply with standard specifications of IS 383:2016 [64]. For recycled aggregate concrete, tested concrete specimens are crushed

through a jaw crusher and sieved to obtain aggregates with a nominal maximum size of 10 mm. The obtained recycled coarse aggregates are used without any treatment in their virgin form. The properties of aggregates are presented in Table 2. Figure 1 illustrates the gradation curve of river sand and CRF.

Table 2. Physical properties of aggregates.

Aggregate	Specific Gravity	Water Absorption (%)	Fineness Modulus
Natural coarse aggregate	2.72	0.10	-
River sand	2.65	0.50	3.62
Crushed rock fines	2.65	0.36	2.89

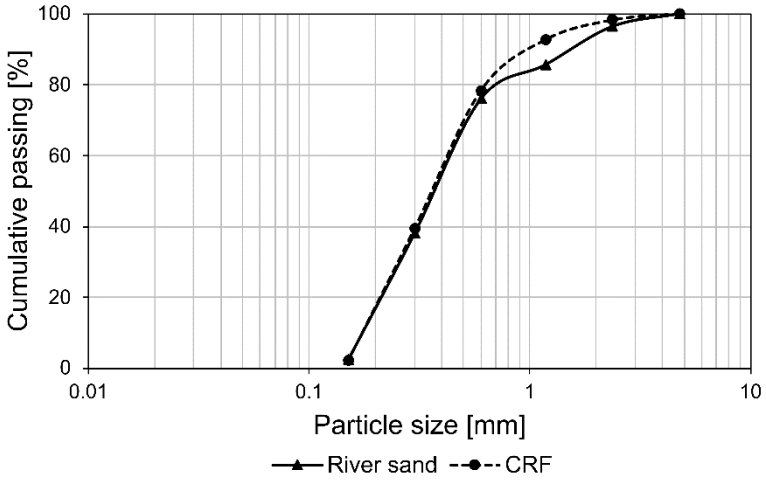

Figure 1. Grading curves of fine aggregates.

As activators, sodium silicate (29.4% SiO_2, 14.7% Na_2O, and 55.9% H_2O) and sodium hydroxide (food-grade, 99% purity) from Hychem Laboratories are utilized in the preparation of AAC mixes.

A denitrifying bacterium *Pseudomonas putida* GAP P-45 purchased from the Microbial Type Culture Collection and Gene Bank (MTCC) Chandigarh is used in BC mixes. Commercially available nutrient broth with 15 g peptone, 3 g yeast extract, 1 g glucose, and 6 g NaCl acquired from Hychem Laboratories is used as the culture medium to cultivate the bacteria. Calcium formate and calcium nitrate obtained from Krishna Chemicals are used as nutrients for bacteria.

Polycarboxylic ether (PCE)-based superplasticizer supplied by BASF is used. Regular tap water free from any deleterious materials is used in concrete mix preparation.

2.2. Mix Proportions

In the present study, three different types of concrete mixes are prepared: AAC, BC, and PCC. Furthermore, by varying mix proportions, 3 AAC mixes and 2 BC mixes are investigated. The details of the mixes are provided in Table 3.

The mixes are selected in such a way that they have equivalent or comparable compressive strength. AAC mixes are denominated based on their activator modulus (ratio of SiO_2/Na_2O in the activating solution). AAC-0.7 has only fly ash as a precursor with an activator modulus of 0.7. In contrast, AAC-1 and AAC-1.4 have fly ash and slag as precursors with activator modulus of 1 and 1.4, respectively. AAC-R has a similar mix proportion to AAC-1.4, with 50% of natural coarse aggregates replaced with RCA. The water content is reduced to ensure sufficient strength development, and hence the workability is improved by PCE-based SP.

Table 3. Mix proportions of AAC, BC and PCC, in [kg/m^3].

Mix	AAC-0.7	AAC-1	AAC-1.4	AAC-R	BC-N	BC	PCC
Fly ash	425.00	280.00	280.00	280.00	115.00	115.00	-
Slag	-	120.00	120.00	120.00	-	-	-
PC	-	-	-	-	335.00	335.00	450.00
Sodium silicate	70.13	115.07	129.43	129.00	-	-	-
Sodium hydroxide	25.08	24.93	10.57	10.60	-	-	-
CRF	-	-	-	-	750.00	750.00	-
River sand	676.49	651.00	651.00	653.00	-	-	623.00
Calcium nitrate	-	-	-	-	4.78	-	-
Calcium formate	-	-	-	-	11.96	-	-
Coarse aggregate	1014.74	1209.00	1209.00	645.00	1020.00	1020.00	1084.00
RCA	-	-	-	645.00	-	-	-
Nutrient broth	-	-	-	-	0.67	0.67	-
Water	68.06	85.37	77.38	67.60	157.00	157.00	150.00
SP	-	-	-	3.14	2.00	2.00	-
Density	2280	2485	2477	2553	2396	2380	2307

PC—Portland cement; CRF—Crushed rock fines; RCA—Recycled coarse aggregate; SP—Superplasticizer.

2.3. Methods

2.3.1. Preparation of Alkali-Activated Concrete Specimens

The activator with a combination of sodium silicate solution and sodium hydroxide pellets is prepared a day before the casting in order to allow sufficient time for heat dissipation. The mixing procedure is commenced with batching, followed by blending of dry materials, viz., coarse aggregates, fine aggregates, and precursors (fly ash and/or slag) in the order mentioned. The uniform blending of dry ingredients is followed by the gradual addition of activator with simultaneous mixing. A measured quantity of additional water is then added and mixed to obtain a homogenous mixture. Specimens are cast in three approximately equal layers, and each layer is compacted using a needle vibrator. The surface of the specimens is finished using a trowel. Molds are then sealed with a plastic sheet to minimize moisture loss. Throughout this study, all the AAC specimens are allowed to cure for at least 24 h in the molds.

The time for demolding the specimens is varied depending on the fly ash content in the mix, owing to its slow reactivity. All the specimens are demolded after gaining sufficient strength to prevent any damage. The AAC-0.7 specimens are demolded at the age of 7 days, as they exhibited the slowest final setting times. AAC-1, AAC-1.4, and AAC-R specimens are demolded at the age of 2 days. On demolding, the specimens are cured until 7-day age underwater and then under ambient laboratory conditions until the commencement of tests. The average ambient temperature was 25 °C, and the relative humidity was in the range of 60–75% in Hyderabad during the experimental activities. This curing regime is selected based on the recommendations of previous research on blended AAC [65,66].

2.3.2. Preparation of Bacterial Concrete Specimens

Bacterial Growth Conditions and Gram Staining

The culture medium and all the related equipment are sterilized in an autoclave at 121 °C for 30 min. The sterilized culture medium is then inoculated with the activated bacterial strain and then placed in an incubator operating at 170 rpm and 37 °C for 24 h. The bacterium is further sub-cultured before being inoculated into the sterilized nutrient broth solution and cultured for 24 h under optimal growth conditions. During this time, the bacterial cell concentration is ensured through the optical density/absorbance at 600 nm (OD_{600}) of the culture broth at regular intervals.

Gram staining is a technique used to distinguish between Gram-positive and Gram-negative bacteria based on the physical and chemical characteristics of their cell walls. The current study utilizes a Gram-negative bacterial strain, and this test is performed to ensure

that the culture did not include any Gram-positive or other microorganisms. Gram staining is dependent on the bacteria's ability to preserve their original color, which is dependent on the cell wall structure. Gram-positive bacteria are characterized by periwinkle color, whereas Gram-negative are characterized through amaranth color [67]. The test procedure commenced by placing the bacteria from the prepared culture on a clean glass slide with a sterile loop. Following this, the slide is heat-fixed by running it over the flame multiple times while ensuring maintenance of the appropriate temperature range. Care is taken to avoid excessive heating as it can result in staining abnormalities and disrupt the morphology of cells. This is followed by four steps of staining. In the first step, the slide is flooded with crystal violet ($C_{25}N_3H_{30}Cl$) for 60 s and then washed with tap water. Step 2 entails exposing the slide to Gram's iodine for 90 s to bind and encapsulate the crystal violet in the cell, followed by washing the slide with tap water. The third step is to destain the smear with 95% ethanol until the thinnest sections of the smear become colorless before rinsing it with water. The fourth step includes flooding the slide with safranin (pink color) for 60 s and rinsing with tap water. Then, the slide is allowed to air-dry. The recorded micrograph of Gram-negative bacteria is presented in Figure 2.

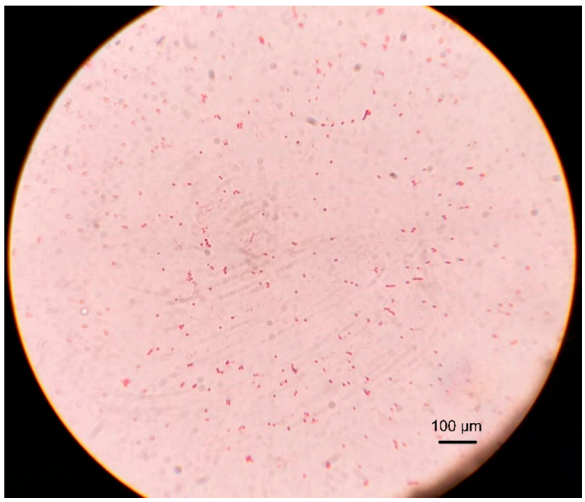

Figure 2. Gram staining of *Pseudomonas putida*.

Casting

The coarse aggregates, CRF, PC, and fly ash are dry mixed, followed by addition of nutrients (calcium nitrate and calcium formate). The required quantities of nutrients are added in case of BC-N mix, while a part of the water is replaced by bacterial solution with the proviso that the water-to-cement ratio is maintained. The specimens are cast following a similar procedure as AAC mixes and cured in water for 28 days until testing.

The preparation of PCC specimens is similar to BC mixes, except for the mixing water free from bacteria and nutrients.

2.3.3. Compressive Strength

The test procedure complies with ASTM standard [68] regulations and is performed on a HEICO compression testing machine (CTM) with a capacity of 2000 kN. The specimens are ensured to surface dry before testing. The specimens are tested in a load control set-up at a loading rate of 0.25 ± 0.05 MPa/s.

2.3.4. Life Cycle Assessment (LCA)

Goal and Scope

The primary aim of this study is to evaluate and compare the environmental impact of preparing different sustainable concrete mixes. The environmental impacts are evaluated for a functional unit of 1 m^3 of concrete with equivalent 28-day compressive strengths

in the range of 40–57 MPa. The mix selection also entails an equivalent curing regime, viz., curing under ambient conditions (20–27 °C) and relative humidity of 60–100%. Seven concrete mixes are evaluated for their environmental impact using cradle-to-gate life cycle assessment (LCA). These seven mixes are: (i) AAC with fly ash as a precursor, activator modulus of 0.7 and a water–solids ratio of 0.2; (ii) AAC with fly ash and slag as precursors, activator modulus of 1 and a water-to-solids ratio of 0.3; (iii) AAC with fly ash and slag as precursors, activator modulus of 1.4 and a water-to-solids ratio of 0.3; (iv) AAC-1.4 with equal proportions of natural and recycled coarse aggregates; (v) BC with nutrients, calcium nitrate and calcium formate; (vi) BC without nutrients, calcium nitrate and calcium formate; (vii) PCC.

In this study, the cradle-to-gate LCA technique is used, including estimations of all emissions and energy consumption from raw material acquisition through concrete preparation. As the major goal of this study is to compare different sustainable concrete mixes, the consumption and disposal phases are not studied, and the environmental effect from these phases is presumed to be similar. The analysis is performed using openLCA v.1.10.3. The system boundary for the mixes investigated in this study from cradle-to-gate is presented in Figure 3.

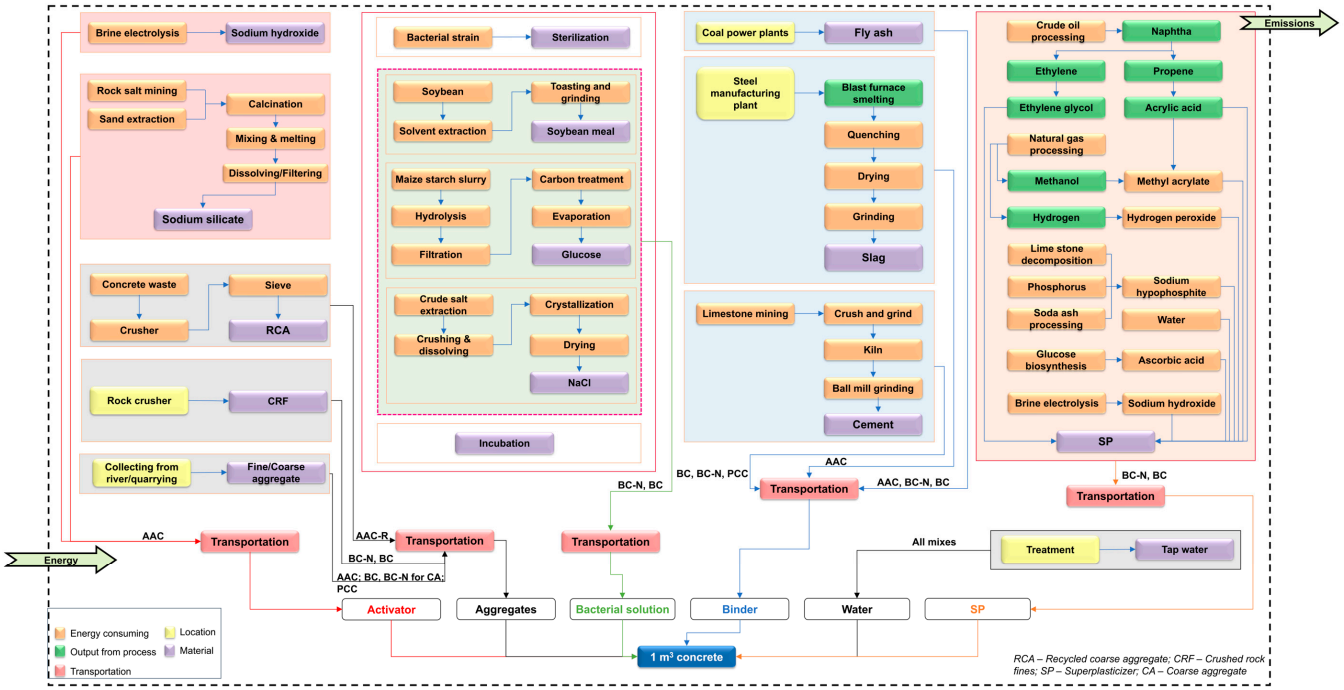

Figure 3. System boundary for cradle-to-gate LCA.

Life Cycle Inventory Analysis

The required data to perform LCA are categorized into two groups: the data associated with emissions and energy consumptions of materials and transportation specified in the system boundary, and those related to electricity consumption associated with RCA and sterilization and incubation associated with preparing the bacterial solution. The emission and energy consumption data for the materials available in the Ecoinvent database (v. 3.7.1) are used [69]. The electricity consumption is calculated based on the specification of the equipment used and the duration or quantity of material processed depending on its energy consumption. The calculated electricity consumption for the services used in the present study is listed in Table 4. The energy consumption per unit quantity (jaw crusher) or time (autoclave and incubator) provided by the manufacturer in the datasheet is used.

Table 4. Energy consumption data of services.

Service	Electricity Consumption (kWh)
Jaw crusher	1.61
Autoclave	1.00
Incubator	4.08

The data for yeast extract are not available in the Ecoinvent database; hence, an alternative for yeast extract production is used in the present study. Previous studies using yeast extract as one of the ingredients show that soybean meal is a potential alternative compared to other alternatives such as fish-powder waste, white gluten waste, perilla meal, sesame meal, and wheat bran [70,71]. Furthermore, the energy consumption per unit (kg) production of soybean meal and yeast extract are approximately equivalent [72,73]. Therefore, soybean meal is used to simulate the energy consumption by yeast extract production in the present study. The environmental burden associated with peptone production is not considered in this study as per the recommendations in the existing literature [74]. Table 5 presents the freight distances and unit cost of raw materials used in the current study in INR. The transportation distances are calculated from the source of their manufacturing to the laboratory where specimens are prepared.

Table 5. Freight distances and unit cost of raw materials and services.

Raw Material	Distance (km)	Cost/kg (Including Freight, INR)
Fly ash	202.0	4.8
Slag	438.0	6.6
PC	231.0	8.3
Sodium silicate	22.8	80.2
Sodium hydroxide	28.4	106.2
CRF	24.2	0.7
River sand	217.0	1.5
Calcium nitrate	22.8	210.0
Calcium formate	22.8	96.0
Coarse aggregate	24.2	1.8
RCA	-	-
Nutrient broth	29.2	2800.0
Water	-	0.035
SP	39.7	232.5
Electricity	-	6.7

The cost of electricity and water is obtained by the guidelines issued by Telangana State Electricity Regulatory Commission, an Indian government regulatory body. The tariff charge per unit of energy consumption (kWh) for industries or commercial use is INR 6.70 [75].

Life Cycle Impact Assessment

The environmental impact of a product is quantified through life cycle impact assessment (LCIA) [76]. ReCiPe 2016, following a hierarchist perspective, is used in the present study. Eleven midpoint indicators are evaluated in this study, which includes global warming potential (GWP), fossil depletion potential (FDP), freshwater ecotoxicity (FETP), freshwater eutrophication (FEP), human toxicity potential (HTP), marine ecotoxicity potential (METP), marine eutrophication potential (MEP), ozone depletion potential (ODP), photochemical oxidant formation potential (POFP), terrestrial acidification potential (TAP), and terrestrial ecotoxicity potential. The endpoint assessment includes three areas of protection, viz., quality of ecosystem, human health, and resource depletion. The openLCA v 1.10.3, an open-source software developed by Hildenbrand et al. [77], is used to evaluate the impacts for each product within the system boundary.

3. Results

3.1. Compressive Strength

The compressive strength of different mixes used in the present study is illustrated in Figure 4. The overall standard deviation in the compressive strength of different mixes is 5.50. Hence, the selected mixes are categorized as having equivalent or comparable compressive strength.

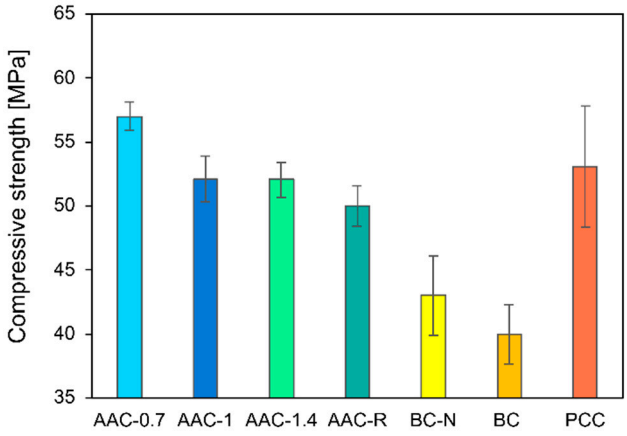

Figure 4. Compressive strength test results.

3.2. Life Cycle Assessment

3.2.1. Midpoint Assessment

Figure 5 presents the results from midpoint impact assessment using ReCiPe 2016 v1.13. It is observed that of all the materials and services considered for four AAC mixes in the present study, transportation followed by sodium silicate contributed the most to climate change. The contributions from transportation and sodium silicate for different AAC mixes vary in the range of 46–53% and 33–21%, respectively. A lower contribution from sodium silicate is identified in AAC-0.7, owing to a lower quantity of sodium silicate compared to the other three AAC (AAC-1, AAC-1.4, and AAC-R) mixes. Transportation entails the combustion of fossil fuels, which results in the release of GHG emissions to the environment. The primary pollutants released due to the combustion of fuels are GHG emissions (CO_2, CH_4, N_2O), ozone precursors (CO, NO_x, non-methane volatile organic compounds (NMVOCs)), particulate matter, and toxic materials (furans and dioxins) [78].

In addition to climate change, transportation is the primary contributor to fossil depletion (51–57%), marine eutrophication (46–52%), photochemical oxidant formation (61–67%), terrestrial acidification (47–53%), and terrestrial ecotoxicity (66–73%) in AAC mixes. Fossil depletion due to transportation is attributed to the use of fuels. In the case of marine eutrophication, excess availability of nitrogen and/or phosphorus can increase phytoplankton production, disrupt the energy balance of the marine ecosystem, and result in the acidification of the ocean [79]. Fossil fuel combustion during transportation releases NO_x in addition to other pollutants. If released in higher quantities, NO_x can contribute to the formation of smog and acid rain, subsequently redepositing to the land and/or aquatic ecosystems [80]. The higher contribution of transportation to photochemical oxidant formation is due to the release of NMVOCs. These pollutants, released due to the partial combustion of fuel, react with nitrogen oxide in the presence of light, resulting in the formation of photochemical ozone [81]. Acidification is caused by air pollutants such as SO_2, NH_3, and NO_x acidifying rivers/streams and soil. These pollutants are also released during the combustion of fossil fuels during transportation. Acidification aggravates trace metal mobilization and leaching in soil, causing harm to aquatic and terrestrial animals and plants by disrupting their energy balance [82]. Terrestrial ecotoxicity is ascribed to the release of heavy metals by road transportation. It is reported in the literature that one of the significant sources of heavy metal emissions to the environment is road transportation. The

major sources of heavy metal emissions from road transportation include three sources of tailpipe emissions: (i) the attrition of engines or after-treatment systems, (ii) lubricants, and (iii) fuel, and non-tailpipe emissions from the attrition of tires or brakes, and road abrasion. In the present investigation, it is identified that petrol (*petrol, low sulfur: ecoinvent 3.7.1*) is the primary source of these trace metal emissions to the environment. The primary trace metals due to road transportation include arsenic (As), lead (Pb), selenium (Se), chromium, copper (Cu), cadmium (Cd), zinc (Zn), and mercury (Hg) [83].

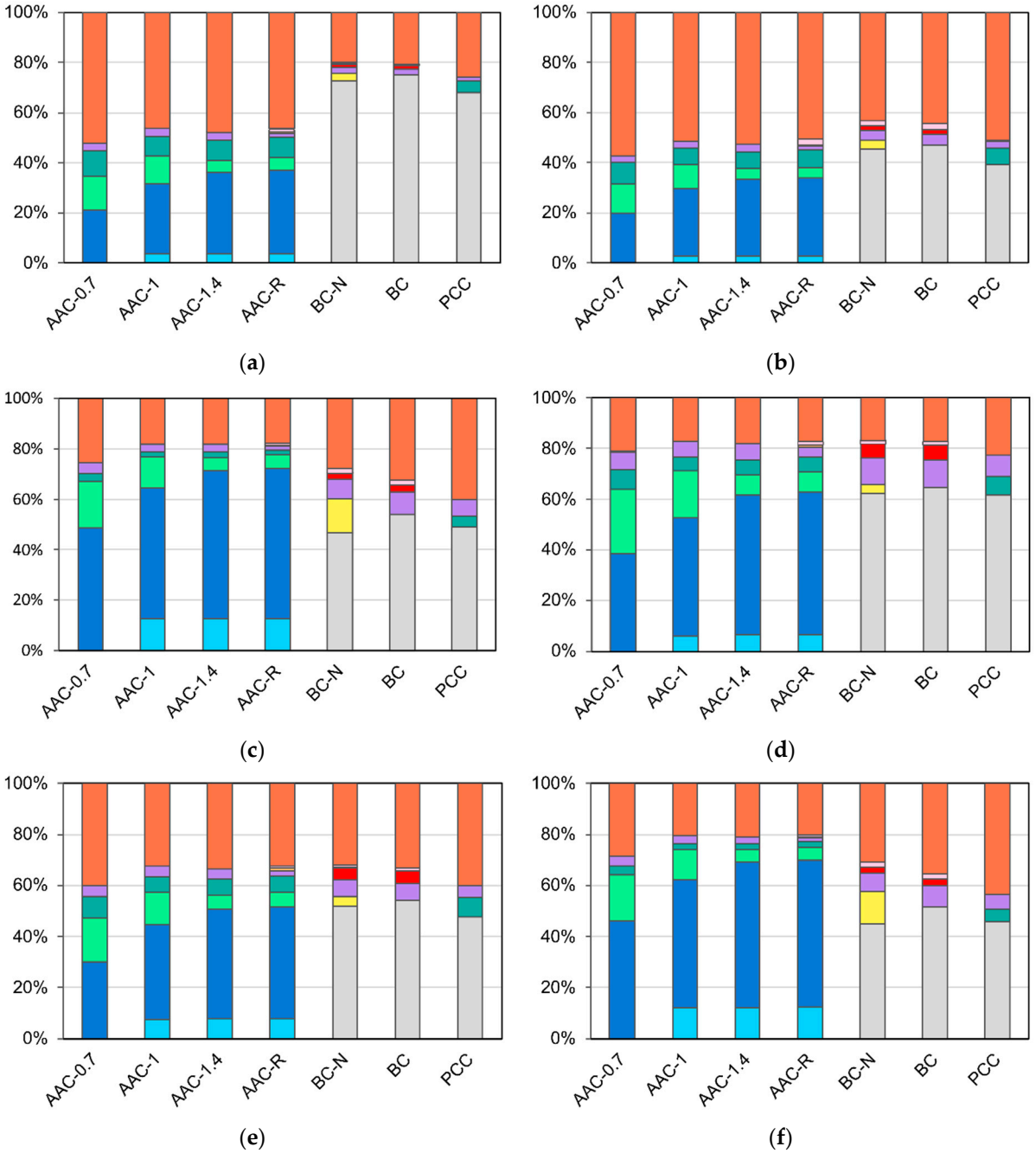

Figure 5. *Cont.*

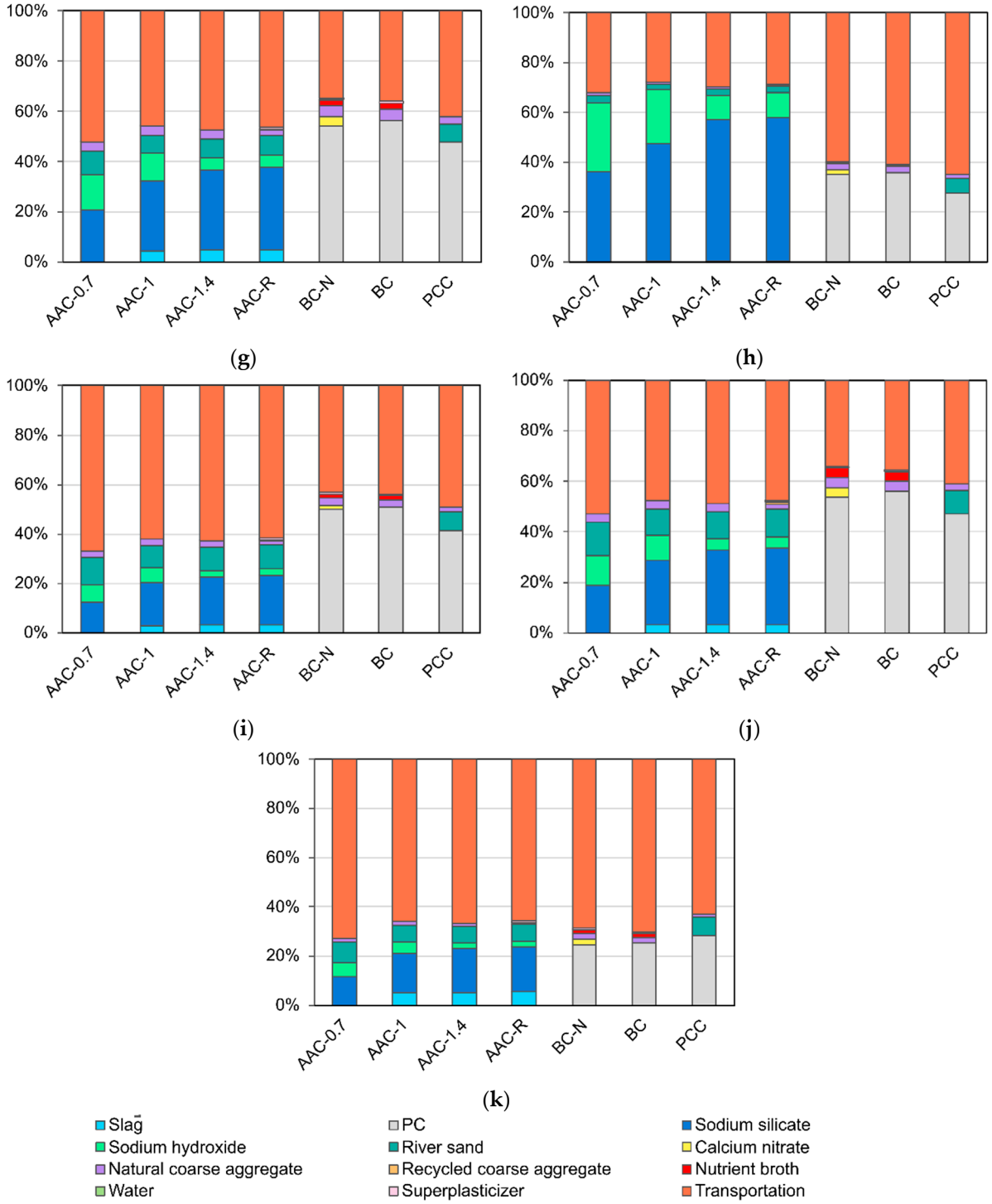

Figure 5. Environmental impacts (%) of different concrete mixes on midpoint damage categories: (**a**) Climate change, (**b**) Fossil depletion, (**c**) Freshwater ecotoxicity, (**d**) Freshwater eutrophication, (**e**) Human toxicity, (**f**) Marine ecotoxicity, (**g**) Marine eutrophication, (**h**) Ozone depletion, (**i**) Photochemical oxidant formation, (**j**) Terrestrial acidification, and (**k**) Terrestrial ecotoxicity.

The other significant contributor to the environmental impact of AAC mixes is sodium silicate, as identified from Figure 5. The contribution of sodium silicate varies in the range of 49–59% for freshwater ecotoxicity, 39–56% for freshwater eutrophication, 30–44% for human toxicity, 46–57% for marine ecotoxicity, and 36–57% for ozone depletion. The hydrothermal dissolution of silica sand in sodium hydroxide solution used to produce sodium silicate is considered in the present study. The procedure is carried out in an auto-

clave, followed by filtration. The production process of sodium silicate entails substantial energy consumption, which is reported as approximately 1.5 kWh/kg for the hydrothermal process [84]. The principal cause of the aforementioned environmental impacts by sodium silicate is electricity consumption during the manufacturing process of sodium silicate and sodium hydroxide (utilized as one of the raw materials for sodium silicate manufacture). In the present study, electricity generated by coal combustion is selected. Coal-fired electricity generation plants release trace metals, SO_2, NO_2, and particulate matter ($PM_{2.5}$) [85]. The principal source for ecotoxicity (freshwater and marine) is trace metals comprising Hg, As, Se, Pb, Cd, and Cr, of which Hg is of critical concern. Coal-fired power plants account for more than one-third of all mercury emissions attributed to human activities [86]. The release of SO_2, NO_2, and $PM_{2.5}$, in addition to trace metals, affects human health. The ozone depletion contributed by sodium silicate is also due to electricity consumption. Mining, plant operation, and the emission of halons 1211, 1301 used as fire suppressants and coolants in gas pipeline distribution all contribute to ozone depletion from coal-fired power plants [87].

PC is the principal contribution from the mixes BC-N, BC, and PC to climate change (68–75%), fossil depletion (39–47%), freshwater ecotoxicity (46–54%), freshwater eutrophication (62–65%), human toxicity (47–54%), marine ecotoxicity (46–52%), marine eutrophication (48–56%), photochemical oxidant formation (41–51%), and terrestrial acidification (47–56%). The calcination phase of PC production results in about 0.525 kg/kg of CO_2 emissions. However, depending on the clinker/PC ratio, the emissions ratio can vary between 0.5 and 0.95, and the remainder is attributed to fuel and electricity consumption [88]. The fossil depletion by PC production can be attributed to the utilization of natural resources as raw materials and fuel consumption. The emissions contributing to ecotoxicity (freshwater and marine) and human toxicity are trace metals, volatile organic compounds (VOCs), dioxins, and particulate matter. Raw materials and fuel are sources for trace metals, and an incomplete combustion of fuel results in the emission of VOCs. The sources of particulate matter include raw material crushing, grinding and drying facilities, clinker combustion process, PC grinding, and the dispatch of PC [89]. Marine eutrophication is primarily caused by NO_x emitted during the production of PC.

However, transportation is responsible for most of the ozone depletion (61–65%) and terrestrial ecotoxicity (63–70%) resulting from the preparation of BC-N, BC, and PC mixes. The reasoning behind the contribution of transportation to ozone depletion and terrestrial ecotoxicity is similar to that of AAC mixes. Fuel combustion also releases ozone precursors, NO_x, CO, and hydrocarbons. The following series of reaction equations elucidate the conversion of ozone precursors to ozone.

$$NO_2 + h\nu \rightarrow NO + O$$

$$O + O_2 \rightarrow O_3$$

$$NO + HO_2 \rightarrow NO_2 + OH$$

The availability of H_2O is from the oxidation of CO or hydrocarbons.

$$CO + OH \rightarrow CO_2 + H$$

$$H + O_2 \rightarrow HO_2$$

Figure 6 presents the normalized midpoint impact indicators for all the mixes. The ReCiPe normalization factors are provided in Table 6.

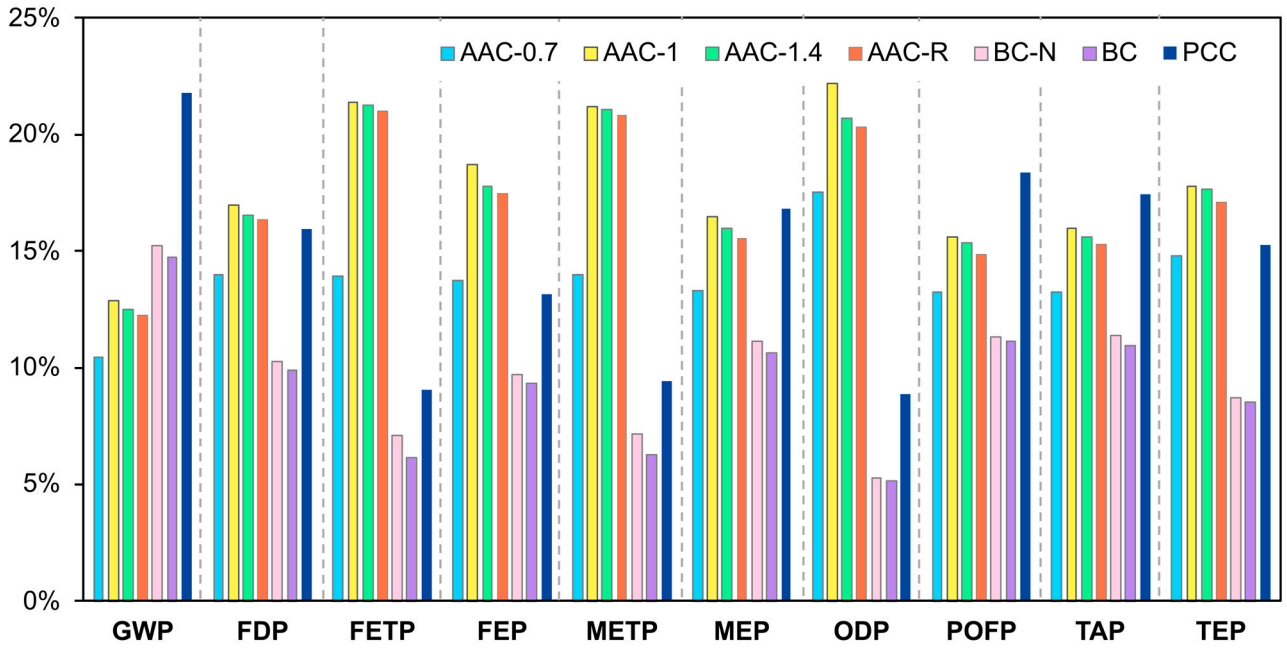

Figure 6. Normalized impacts of different concrete mixes on midpoint damage categories.

Table 6. Normalization scores for ReCiPe 2016 methodology [90].

Indicator	ReCiPe Midpoint (H)
GWP	5.51×10^{13}
FDP	3.93×10^{12}
FETP	1.74×10^{11}
FEP	4.48×10^{9}
HTP-cancer	7.10×10^{10}
HTP-no cancer	2.16×10^{14}
METP	3.00×10^{11}
MEP	3.18×10^{10}
ODP	4.14×10^{8}
POFP	1.42×10^{11}
TAP	2.83×10^{11}
TETP	1.05×10^{14}

The overall contribution of individual blends to the impact categories can be effectively interpreted using Figure 6. The GWP of PC is approximately twice that of AAC-0.7 and 1.4 times that of BC-N. AAC-0.7 has lower environmental impacts among the AAC mixes across all the impact categories. This is attributed to a lower content of alkaline activators, viz., sodium silicate and sodium hydroxide used in AAC-0.7 compared to other AAC mixes. AAC-1, AAC-1.4, and AAC-R show the highest environmental impacts for all the damage categories, excluding POFP and TAP. This is ascribed to the manufacturing process of sodium silicate and sodium hydroxide. Furthermore, there is negligible variance in the impacts exhibited by these three mixes due to the usage of an equivalent number of activators. BC-N and BC have lower environmental impacts for all the damage categories, excluding GWP. The higher GWP of BC-N and BC is attributed to the use of PC as the binder. The lower impacts for all the other damage categories are attributed to two factors: the usage of a lower PC content (335 kg/m^3) compared to PCC (450 kg/m^3) and the complete replacement of silica sand with CRF as fine aggregates. The CRF are not allotted any environmental burden in the present study and are considered as waste generated from the stone grinding. Furthermore, the usage of CRF eliminates the environmental impacts associated with the mining of sand from natural reserves.

PCC has the highest POFP and TAP in addition to GWP. The calcination phase in the production of PC is the primary supplier of CO_2 emissions and consequently to climate change. A reported quantity of 0.525 kg CO_2/kg of clinker is produced during the decarbonization of limestone in the kiln. The fuel and electricity consumption result in 0.335 kg CO_2 and 0.05 kg CO_2 emissions per kg of cement [91]. The VOCs emitted during incomplete combustion contribute to photochemical oxidant formation, whereas NO_x, SO_x and their associated compounds contribute to terrestrial acidification. Approximately 0.0023–0.138 kg VOCs/tonne of clinker are emitted due to the incomplete combustion of fuel during PC production [89]. NO_x and other nitrogen compounds are released when a fuel nitrogen combines with oxygen in the flame, or due to a combination of ambient nitrogen and oxygen in the combustion air. The nitrogen-related emissions are in the range of 0.33–4.67 kg/tonne of clinker. The source of SO_x and other sulfur compounds is fuel and raw materials with a high volatile sulfur content, and their emissions are in the range of 11.12 kg/tonne of clinker.

3.2.2. Endpoint Assessment

Figure 7 presents the endpoint assessment of different AAC, BC and PCC mixes used in the present study.

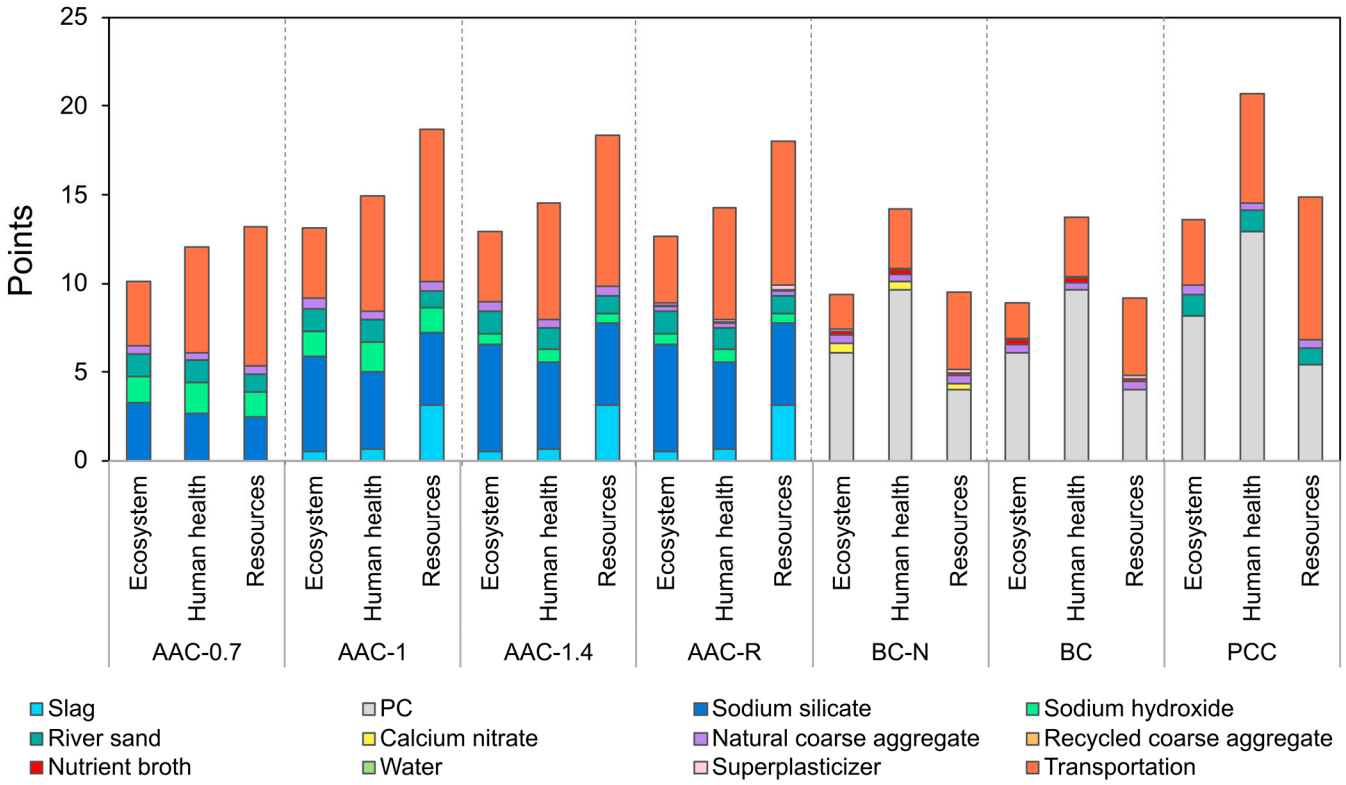

Figure 7. Endpoint environmental impact assessment of different concrete mixes.

The production of all the AAC and BC mixes has a lower negative impact on the quality of the ecosystem than PCC. The ecosystem quality value of AAC mixes ranges between 10.12 (AAC-0.7) and 13.09 (AAC-1). In contrast, PCC has a value of 13.59, which is 25.6% and 3.6% higher than AAC-0.7 and AAC-1, respectively. The emissions from the production process of PC have a detrimental effect on ecosystem quality, whereas in AAC mixes, sodium silicate followed by transportation (service) contribute adversely to the ecosystem quality. Of all the mixes, BC exhibited a lower impact on the quality of the ecosystem, with an endpoint value of 8.91, which is 34.4% lower than PC. The raw materials and/or services contributing to the GWP, FEP, FETP, TETP, TAP, and METP are associated with ecosystem quality.

PCC has the highest impact on human health with an endpoint value of 20.69, followed by AAC-1 with an endpoint value of 14.96. As evident from Figure 7, about 62.5% of the total impact on human health is caused by the use of PC and 29.7% by transportation in the PCC mix. In AAC-1, 29.2% of the overall impact on human health is contributed by sodium silicate and about 43.8% by transportation. BC has the lowest impact on human health of all the mixes, with an endpoint value of 13.7, which is 33.8% lower than the PCC mix. The raw materials and/or services considered in the present study and discussed in the midpoint assessment contributing to particulate matter, HTP, and GWP are associated with adverse effects on human health.

AAC mixes show the highest resource depletion compared to other mixes. AAC-1 has the highest resource depletion value of 18.66, of which 45.8% is contributed by transportation and 21.8% by sodium silicate. The endpoint values of AAC-1 and AAC-1.4 differ only by 1.5%; however, this difference is attributed to sodium hydroxide. The electrolytic phase of the chloralkali process using diaphragm technology to produce sodium hydroxide is reported to consume 2.97 kWh/kg of electricity [92]. This electricity consumption by the manufacturing process of sodium hydroxide is approximately thrice as high as PC and twice as high as sodium silicate production. When individually considered, the environmental impact due to the production of sodium hydroxide is higher than sodium silicate. However, due to its usage in lower quantities in the present study, the effect of sodium hydroxide on different damage categories is minimal. BC has the lowest resource depletion score of 9.14, which is approximately half of ACC-1.

When an individual type of concrete mix is considered, AAC-0.7 has the lowest environmental impact on all three areas of protection: ecosystem quality, human health, and resource depletion of all the AAC mixes. This is attributed to the lower quantity of sodium silicate used in AAC-0.7 compared to other AAC mixes. In the case of BC mixes, due to eliminating environmental impacts associated with the use of calcium nitrate and calcium formate, BC exhibited lower environmental impacts on all three areas of protection. When all the mixes in the present study are considered, BC exhibits the lowest environmental impact. Despite the similar binder used in BC and PCC mixes, the lower environmental impacts by BC are attributed to the lower PC content, the complete replacement of sand with CRF, and the transportation effect. Though in the case of BC the number of raw materials is higher compared to PCC, the overall quantity multiplied by a distance given as input to transportation is approximately half (45.8% lower) of the PCC mix.

3.3. Economic Assessment

A sustainable concrete mix should also be economically viable to promote its in situ applications and commercial use. Therefore, a cost analysis is performed for the mixes investigated in the present study and the results are presented in Figure 8.

The cost of AAC mixes ranging between INR 13172 and INR 17168 is 98.8–159.1% higher than PCC. BC mixes have an overall cost of INR 8074–10226, which is approximately 21.8–54.3% higher than PCC. Sodium silicate used in AAC contributes to 42.7–62.7%, lowest in AAC-0.7 and highest for AAC-1.4. Though the unit cost of sodium hydroxide is high, the higher contribution from sodium silicate is attributed to its higher proportion in these mixes. Analogously, owing to higher quantities of sodium hydroxide in AAC-0.7 and AAC-1, its contribution to the total cost is 20.2% and 15.4%, respectively. The contribution from PC ranging between 27.2% and 34.4% is highest in BC-N and BC mixes. The coarse aggregates and nutrient broth result in 17.9–22.7% and 18.3–23.2%, respectively. Since the overall cost of BC mix is lower than BC-N (by 21.0%) owing to the omission of nutrients, the contribution from coarse aggregates and nutrient broth is higher in the BC mix. Calcium nitrate and calcium formate together account for 21.0% of the overall cost of the combination, with approximately equal individual contributions. The cost of water and electricity is negligible compared to raw materials and transportation.

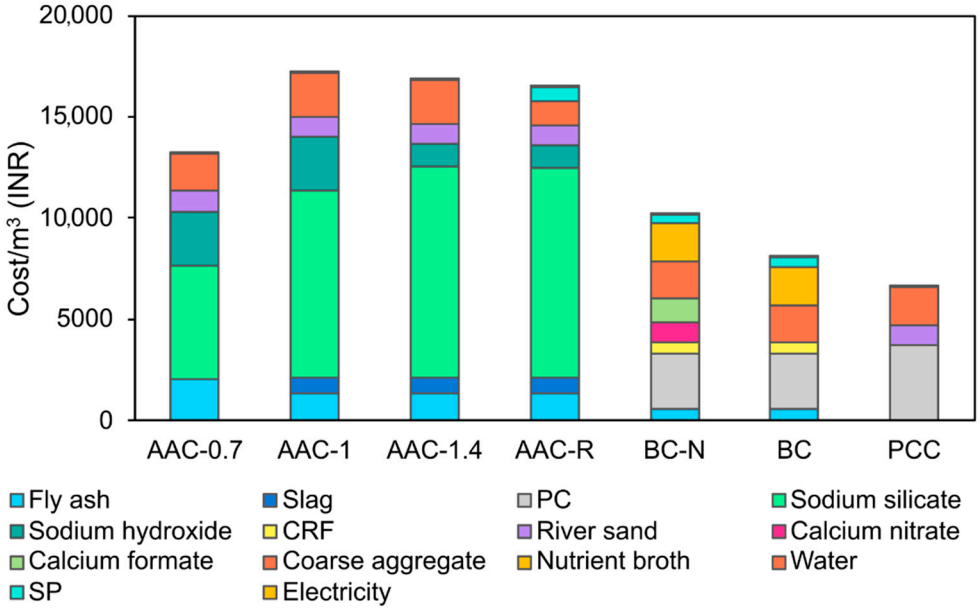

Figure 8. Cost estimate of different concrete mixes.

4. Conclusions

This study performs a comprehensive life cycle assessment of three different sustainable concrete mixes: (1) alkali-activated concrete (AAC) with natural coarse aggregates, (2) AAC with recycled coarse aggregates, and (3) bacterial concrete (BC). All the selected mixes are compared for their environmental impact versus Portland cement concrete (PCC) of equivalent strength. The environmental implications of three different AAC mixes with natural coarse aggregates and two different BC mixes (with and without nutrients) are evaluated as a function of mix proportions. A simplified cost analysis is performed in the Indian context. The findings are summarized as follows:

- For different AAC mixtures, contributions from transportation and sodium silicate are the highest for different midpoint damage categories.
- Portland cement is the principal contributor from the BC and PCC mixes to various midpoint damage categories.
- PCC has a GWP that is almost twice that of AAC with an activator modulus of 0.7 (AAC-0.7) and 1.4 times that of BC with nutrients.
- Owing to lower quantities of alkaline activators and only fly ash as a precursor, AAC-0.7 has the lowest environmental impact of all AAC mixes. The electricity consumption by recycled coarse aggregates (RCA) increased the environmental impact caused by AAC with RCA.
- PCC and AAC with an activator modulus of 1 (AAC-1) have the most detrimental effect on the quality of ecosystems and human health. AAC-1 has the highest resource depletion value (18.66) of all the mixes.
- BC (bacterial concrete without nutrients) has the lowest environmental effect of the evaluated mixes for all midpoint damage categories except GWP and endpoint damage categories. BC has the lowest resource depletion value (9.14), which is almost half of ACC-1.
- The cost of AAC mixes is 98.8–159.1%, and the cost of BC mixes is 21.8–54.3% higher than PCC.
- Sodium silicate in AAC mixes, PC, coarse aggregates, and nutrient broth in BC mixes have the highest contribution to the total cost.

The present study provides a detailed LCA of bacterial concrete, which is not reported in the existing literature. A comprehensive comparison of the environmental impact of different concrete mixes at midpoint and endpoint damage levels and a cost analysis would assist the industry and policymakers in identifying a viable, sustainable alternative.

Author Contributions: Conceptualization, K.K.R. and A.K.; methodology, K.K.R.; software, K.K.R. and R.C.; validation, K.K.R., R.C. and R.K.B.; formal analysis, K.K.R., R.C., and A.K.; investigation, K.K.R., R.C. and R.K.B.; data curation, K.K.R., R.C., R.K.B., and A.K.; writing—original draft preparation, K.K.R. and A.K.; writing—review and editing, P.K.D.M.; supervision, A.K. All authors have read and agreed to the published version of the manuscript.

Funding: This research received no external funding.

Institutional Review Board Statement: This study does not involve any studies on humans or animals.

Informed Consent Statement: Not applicable.

Data Availability Statement: All data, models, and code generated or used during the study appear in the submitted article. Some or all data, models, or code that support the findings of this study is available from the corresponding author upon reasonable request.

Conflicts of Interest: The authors declare no conflict of interest.

References

1. Rogelj, J.; Shindell, D.; Jiang, K.; Fifita, S.; Forster, P.; Ginzburg, V.; Handa, C.; Kheshgi, H.; Kobayashi, S.; Kriegler, E.; et al. *Global Warming of 1.5 °C—Chapter 2 Mitigation Pathways Compatible with 1.5 °C in the Context of Sustainable Development*; Intergovernmental Panel on Climate Change: Geneva, Switzerland, 2018; pp. 93–174.
2. Keith, D.W.; Holmes, G.; Angelo, D.S.; Heidel, K. A process for capturing CO_2 from the atmosphere. *Joule* **2018**, *2*, 1573–1594. [CrossRef]
3. UNEP. Building Sector Emissions Hit Record High, but Low-Carbon Pandemic Recovery Can Help Transform Sector. Available online: https://www.unep.org/news-and-stories/press-release/building-sector-emissions-hit-record-high-low-carbon-pandemic (accessed on 15 June 2021).
4. UNFCCC. *Adoption of the Paris Agreement*; United Nations Framework Convention on Climate Change: Geneva, Switzerland, 2015. Available online: https://unfccc.int/sites/default/files/english_paris_agreement.pdf (accessed on 15 June 2021).
5. Huang, L.; Krigsvoll, G.; Johansen, F.; Liu, Y.; Zhang, X. Carbon emission of global construction sector. *Renew. Sustain. Energy Rev.* **2018**, *81*, 1906–1916. [CrossRef]
6. Benhelal, E.; Zahedi, G.; Shamsaei, E.; Bahadori, A. Global strategies and potentials to curb CO_2 emissions in cement industry. *J. Clean. Prod.* **2013**, *51*, 142–161. [CrossRef]
7. Danish, A.; Mosaberpanah, M.A.; Salim, M.U.; Fediuk, R.; Rashid, M.F.; Waqas, R.M. Reusing marble and granite dust as cement replacement in cementitious composites: A review on sustainability benefits and critical challenges. *J. Build. Eng.* **2021**, *44*, 102600. [CrossRef]
8. Rakhimova, N.R.; Rakhimov, R.; Morozov, V.; Eskin, A. Calcined low-grade clays as sources for zeolite containing material. *Period. Polytech. Civ. Eng.* **2021**, *65*, 204–214. [CrossRef]
9. Barbuta, M.; Bucur, R.D.; Cimpeanu, S.M.; Paraschiv, G.; Bucur, D. *Wastes in Building Materials Industry*; IntechOpen: London, UK, 2015; Volume 1, pp. 81–99. [CrossRef]
10. Shao, Y.; Mahoutian, M.; Ghouleh, Z. Carbonation-activated steel slag binder as alternative cementing material. *ACI Spec. Publ.* **2017**, *320*, 21.1–21.14.
11. Marvila, M.T.; Azevedo, A.R.G.D.; Matos, P.R.D.; Monteiro, S.N.; Vieira, C.M.F. Rheological and the fresh state properties of alkali-activated mortars by blast furnace slag. *Materials* **2021**, *14*, 2069. [CrossRef] [PubMed]
12. Ramagiri, K.K.; Kar, A. Effect of high-temperature on the microstructure of alkali-activated binder. *Mater. Today* **2020**, *28*, 1123–1129. [CrossRef]
13. Ramagiri, K.K.; Patil, S.; Mundra, H.; Kar, A. Laboratory investigations on the effects of acid attack on concrete containing portland cement partially replaced with ambient-cured alkali-activated binders. *Adv. Concr. Constr.* **2020**, *10*, 221–236. [CrossRef]
14. Ramagiri, K.K.; Chauhan, D.R.; Gupta, S.; Kar, A.; Adak, D.; Mukherjee, A. High-temperature performance of ambient-cured alkali-activated binder concrete. *Innov. Infrastruct. Solut.* **2021**, *6*, 71. [CrossRef]
15. Torres-Carrasco, M.; Puertas, F. La activación alcalina de diferentes aluminosilicatos como una alternativa al Cemento Portland: Cementos activados alcalinamente o geopolímeros. *Rev. Ing. Constr.* **2017**, *32*, 5–12. [CrossRef]
16. Provis, J.L.; Bernal, S.A. Geopolymers and related alkali-activated materials. *Annu. Rev. Mater. Sci.* **2014**, *44*, 299–327. [CrossRef]
17. Villoria Sáez, P.; Osmani, M. A diagnosis of construction and demolition waste generation and recovery practice in the European Union. *J. Clean. Prod.* **2019**, *241*, 118400. [CrossRef]
18. NITI Aayog. *Resource Efficiency and Circular Economy-Current Status and Way Forward*; National Institution for Transforming India: New Delhi, India, 2019.
19. Akhtar, A.; Sarmah, A.K. Construction and demolition waste generation and properties of recycled aggregate concrete: A global perspective. *J. Clean. Prod.* **2018**, *186*, 262–281. [CrossRef]

20. Pyngrope, M.; Hossiney, N.; Chen, Y.; Thejas, H.K.; Sarath, C.K.; Alex, J.; Lakshmish Kumar, S. Properties of alkali-activated concrete (AAC) incorporating demolished building waste (DBW) as aggregates. *Cogent Eng.* **2021**, *8*, 1870791. [CrossRef]
21. Xiao, J.Z.; Li, J.B. Study on relationships between strength indexes of recycled concrete. *J. Build. Mater.* **2005**, *2*, 197–201. (In Chinese) [CrossRef]
22. Li, X. Recycling and reuse of waste concrete in China: Part I. Material behaviour of recycled aggregate concrete. *Resour. Conserv. Recycl.* **2008**, *53*, 36–44. [CrossRef]
23. Kwan, W.H.; Ramli, M.; Kam, K.J.; Sulieman, M.Z. Influence of the amount of recycled coarse aggregate in concrete design and durability properties. *Constr. Build. Mater.* **2012**, *26*, 565–573. [CrossRef]
24. Liu, Q.; Xiao, J.; Sun, Z. Experimental study on the failure mechanism of recycled concrete. *Cem. Concr. Res.* **2011**, *41*, 1050–1057. [CrossRef]
25. Abdollahnejad, Z.; Mastali, M.; Falah, M.; Luukkonen, T.; Mazari, M.; Illikainen, M. Construction and Demolition Waste as Recycled Aggregates in Alkali-Activated Concretes. *Materials* **2019**, *12*, 4016. [CrossRef]
26. Turner, L.K.; Collins, F.G. Carbon dioxide equivalent (CO_2-e) emissions: A comparison between geopolymer and OPC cement concrete. *Constr. Build. Mater.* **2013**, *43*, 125–130. [CrossRef]
27. Fořt, J.; Vejmelková, E.; Koňáková, D.; Alblová, N.; Čáchová, M.; Keppert, M.; Rovnaníková, P.; Černý, R. Application of waste brick powder in alkali activated aluminosilicates: Functional and environmental aspects. *J. Clean. Prod.* **2018**, *194*, 714–725. [CrossRef]
28. Katz, A. Properties of concrete made with recycled aggregate from partially hydrated old concrete. *Cem. Concr. Res.* **2003**, *33*, 703–711. [CrossRef]
29. Movassaghi, R. Durability of Reinforced Concrete Incorporating Recycled Concrete as Aggregate (RCA). Master's Thesis, University of Waterloo, Waterloo, ON, Canada, 2006. Available online: http://hdl.handle.net/10012/2884 (accessed on 1 June 2021).
30. Mastali, M.; Abdollahnejad, Z.; Pacheco-Torgal, F. 15—Carbon dioxide sequestration of fly ash alkaline-based mortars containing recycled aggregates and reinforced by hemp fibers: Mechanical properties and numerical simulation with a finite element method. In *Carbon Dioxide Sequestration in Cementitious Construction Materials*; Woodhead Publishing: New Delhi, India, 2018; pp. 373–391. [CrossRef]
31. de Juan, M.S.; Gutiérrez, P.A. Study on the influence of attached mortar content on the properties of recycled concrete aggregate. *Constr. Build. Mater.* **2009**, *23*, 872–877. [CrossRef]
32. Abbas, A.; Fathifazl, G.; Burkan Isgor, O.; Razaqpur, A.; Fournier, B.; Foo, S. Proposed Method for Determining the Residual Mortar Content of Recycled Concrete Aggregates. *J. ASTM Int.* **2007**, *5*, 1–12. [CrossRef]
33. Akbarnezhad, A.; Ong, K.C.G.; Zhang, M.H.; Tam, C.T.; Foo, T.W.J. Microwave-assisted beneficiation of recycled concrete aggregates. *Constr. Build. Mater.* **2011**, *25*, 3469–3479. [CrossRef]
34. Yanagibashi, K.; Inoue, K.; Seko, S.; Tsuji, D. A study on cyclic use of aggregate for structural concrete. In Proceedings of the SB05: The 2005 World Sustainable Building Conference, Tokyo, Japan, 27–29 September; pp. 9–11.
35. Shima, H.; Tateyashiki, H.; Matsuhashi, R.; Yoshida, Y. An Advanced Concrete Recycling Technology and its Applicability Assessment through Input-Output Analysis. *J. Adv. Concr. Technol.* **2005**, *3*, 53–67. [CrossRef]
36. Sidiq, A.; Setunge, S.; Gravina, R.J.; Giustozzi, F. Self-repairing cement mortars with microcapsules: A microstructural evaluation approach. *Constr. Build. Mater.* **2020**, *232*, 117239. [CrossRef]
37. Kane, J.W.; Tomer, A. Shifting into an Era of Repair: Us Infrastructure Spending Trends. Brookings. Available online: https://www.brookings.edu/research/shifting-into-an-era-of-repair-us-infrastructure-spending-trends/ (accessed on 15 June 2021).
38. Alves, L.; Alves, L.; Mello, M.; Barros, S.D. Characterization of bioconcrete and the properties for self-healing. *Proceedings* **2019**, *38*, 4. [CrossRef]
39. ONS. Construction Output in Great Britain: May 2016, Office for National Statistics. Available online: https://www.ons.gov.uk/businessindustryandtrade/constructionindustry/bulletins/constructionoutputingreatbritain/may2016 (accessed on 1 June 2021).
40. Best, R.D. Global Investments on the Construction and Maintenance of Infrastructure as Share of GDP in 2018. Available online: https://www.statista.com/statistics/566787/average-yearly-expenditure-on-economic-infrastructure-as-percent-of-gdp-worldwide-by-country/ (accessed on 15 June 2021).
41. Wu, M.; Johannesson, B.; Geiker, M. A review: Self-healing in cementitious materials and engineered cementitious composite as a self-healing material. *Constr. Build. Mater.* **2012**, *28*, 571–583. [CrossRef]
42. Termkhajornkit, P.; Nawa, T.; Yamashiro, Y.; Saito, T. Self-healing ability of fly ash–cement systems. *Cem. Concr. Compos.* **2009**, *31*, 195–203. [CrossRef]
43. Jonkers, H.M.; Thijssen, A.; Muyzer, G.; Copuroglu, O.; Schlangen, E. Application of bacteria as self-healing agent for the development of sustainable concrete. *Ecol. Eng.* **2010**, *36*, 230–235. [CrossRef]
44. De Muynck, W.; De Belie, N.; Verstraete, W. Microbial carbonate precipitation in construction materials: A review. *Ecol. Eng.* **2010**, *36*, 118–136. [CrossRef]
45. Erşan, Y.Ç.; Hernandez-Sanabria, E.; Boon, N.; de Belie, N. Enhanced crack closure performance of microbial mortar through nitrate reduction. *Cem. Concr. Compos.* **2016**, *70*, 159–170. [CrossRef]

46. Zhang, W.; Zheng, Q.; Ashour, A.; Han, B. Self-healing cement concrete composites for resilient infrastructures: A review. *Compos. B. Eng.* **2020**, *189*, 107892. [CrossRef]
47. Achal, V.; Mukerjee, A.; Sudhakara Reddy, M. Biogenic treatment improves the durability and remediates the cracks of concrete structures. *Constr. Build. Mater.* **2013**, *48*, 1–5. [CrossRef]
48. Chahal, N.; Siddique, R.; Rajor, A. Influence of bacteria on the compressive strength, water absorption and rapid chloride permeability of fly ash concrete. *Constr. Build. Mater.* **2012**, *28*, 351–356. [CrossRef]
49. Sonali Sri Durga, C.; Ruben, N.; Sri Rama Chand, M.; Venkatesh, C. Performance studies on rate of self healing in bio concrete. *Mater. Today* **2020**, *27*, 158–162. [CrossRef]
50. Jena, S.; Basa, B.; Panda, K.C.; Sahoo, N.K. Impact of Bacillus subtilis bacterium on the properties of concrete. *Mater. Today* **2020**, *32*, 651–656. [CrossRef]
51. Khaliq, W.; Ehsan, M.B. Crack healing in concrete using various bio influenced self-healing techniques. *Constr. Build. Mater.* **2016**, *102*, 349–357. [CrossRef]
52. Shaheen, N.; Khushnood, R.A.; Ud din, S. Bioimmobilized limestone powder for autonomous healing of cementitious systems: A feasibility study. *Adv. Mater. Sci. Eng.* **2018**, *2018*, 7049121. [CrossRef]
53. Khushnood, R.A.; ud din, S.; Shaheen, N.; Ahmad, S.; Zarrar, F. Bio-inspired self-healing cementitious mortar using Bacillus subtilis immobilized on nano-/micro-additives. *J. Intell. Mater. Syst. Struct.* **2018**, *30*, 3–15. [CrossRef]
54. Manzur, T.; Rahman, F.; Afroz, S.; Huq, R.S.; Efaz, I.H. Potential of a microbiologically induced calcite precipitation process for durability enhancement of masonry aggregate concrete. *J. Mater. Civ. Eng.* **2017**, *29*, 04016290. [CrossRef]
55. Papanikolaou, I.; Arena, N.; Al-Tabbaa, A. Graphene nanoplatelet reinforced concrete for self-sensing structures—A lifecycle assessment perspective. *J. Clean. Prod.* **2019**, *240*, 118202. [CrossRef]
56. Alazhari, M.; Sharma, T.; Heath, A.; Cooper, R.; Paine, K. Application of expanded perlite encapsulated bacteria and growth media for self-healing concrete. *Constr. Build. Mater.* **2018**, *160*, 610–619. [CrossRef]
57. Xu, J.; Wang, X.; Zuo, J.; Liu, X. Self-Healing of Concrete Cracks by Ceramsite-Loaded Microorganisms. *Adv. Mater. Sci. Eng.* **2018**, *2018*, 5153041. [CrossRef]
58. Wang, J.; Van Tittelboom, K.; De Belie, N.; Verstraete, W. Use of silica gel or polyurethane immobilized bacteria for self-healing concrete. *Constr. Build. Mater.* **2012**, *26*, 532–540. [CrossRef]
59. Luo, M.; Qian, C. Influences of bacteria-based self-healing agents on cementitious materials hydration kinetics and compressive strength. *Constr. Build. Mater.* **2016**, *121*, 659–663. [CrossRef]
60. Wang, J.Y.; Soens, H.; Verstraete, W.; De Belie, N. Self-healing concrete by use of microencapsulated bacterial spores. *Cem. Concr. Res.* **2014**, *56*, 139–152. [CrossRef]
61. Paine, K. Bacteria-based self-healing concrete: Effects of environment, exposure and crack size. In Proceedings of the RILEM Conference on Microorganisms-Cementitious Materials Interactions, Delft, The Netherlands, 23 June 2016; Wiktor, V., Jonkers, H., Bertron, A., Eds.; RILEM Publications S.A.R.L.: Paris, France, 2016.
62. BIS. *IS 12269 Ordinary Portland Cement, 53 Grade—Specification*; Bureau of Indian Standards: New Delhi, India, 2013.
63. ASTM. *C150/C150M Standard Specification for Portland Cement*; ASTM International: West Conshohocken, PA, USA, 2020.
64. BIS. *IS 383 Coarse and Fine Aggregate for Concrete—Specification (Third Revision)*; Bureau of Indian Standards: New Delhi, India, 2016.
65. El-Hassan, H.; Ismail, N. Effect of process parameters on the performance of fly ash/GGBS blended geopolymer composites. *J. Sustain. Cem.-Based Mater.* **2018**, *7*, 122–140. [CrossRef]
66. El-Hassan, H.; Shehab, E.; Al-Sallamin, A. Influence of different curing regimes on the performance and microstructure of alkali-activated slag concrete. *J. Mater. Civ. Eng.* **2018**, *30*, 04018230. [CrossRef]
67. Salmasi, F.; Mostofinejad, D. Investigating the effects of bacterial activity on compressive strength and durability of natural lightweight aggregate concrete reinforced with steel fibers. *Constr. Build. Mater.* **2020**, *251*, 119032. [CrossRef]
68. ASTM. *C39/C39M-18 Standard Test Method for Compressive Strength of Cylindrical Concrete Specimens*; ASTM International: West Conshohocken, PA, USA, 2018.
69. Moreno Ruiz, E.; Valsasina, L.; FitzGerald, D.; Symeonidis, A.; Turner, D.; Müller, J.; Minas, N.; Bourgault, G.; Vadenbo, C.; Ioannidou, D.; et al. *Documentation of Changes Implemented in Ecoinvent Database v3. 7 & v3. 7.1*; Ecoinvent Association: Zürich, Switzerland, 2020. Available online: https://www.ecoinvent.org/files/change_report_v3_7_1_20201217.pdf (accessed on 15 June 2021).
70. Sahnoun, M.; Kriaa, M.; Elgharbi, F.; Ayadi, D.-Z.; Bejar, S.; Kammoun, R. Aspergillus oryzae S2 alpha-amylase production under solid state fermentation: Optimization of culture conditions. *Int. J. Biol. Macromol.* **2015**, *75*, 73–80. [CrossRef] [PubMed]
71. Hong, M.; Jang, I.; Son, Y.; Yi, C.; Park, W. Agricultural by-products and oyster shell as alternative nutrient sources for microbial sealing of early age cracks in mortar. *AMB Express* **2021**, *11*, 11. [CrossRef]
72. Kumar, L.R.; Yellapu, S.K.; Zhang, X.; Tyagi, R.D. Energy balance for biodiesel production processes using microbial oil and scum. *Bioresour. Technol.* **2019**, *272*, 379–388. [CrossRef]
73. Hill, J.; Nelson, E.; Tilman, D.; Polasky, S.; Tiffany, D. Environmental, economic, and energetic costs and benefits of biodiesel and ethanol biofuels. *Proc. Natl. Acad. Sci. USA* **2006**, *103*, 11206. [CrossRef]

74. Myhr, A.; Røyne, F.; Brandtsegg, A.S.; Bjerkseter, C.; Throne-Holst, H.; Borch, A.; Wentzel, A.; Røyne, A. Towards a low CO_2 emission building material employing bacterial metabolism (2/2): Prospects for global warming potential reduction in the concrete industry. *PLoS ONE* **2019**, *14*, e0208643. [CrossRef] [PubMed]
75. TSERC. Retail Supply Tariff Order for FY 2018-19—Salient Features. Available online: https://tserc.gov.in/file_upload/uploads/Tariff%20Orders/Tariff%20Schedule/Tariff%20Schedule%20for%20FY2018-19.pdf (accessed on 15 June 2021).
76. BIS. *IS/ISO 14040 Environmental Management: Life Cycle Assessment*; Requirements and Guidelines; Bureau of Indian Standards: New Delhi, India, 2006.
77. Hildenbrand, J.; Srocka, M.; Siroth, A. Why We Started the Development of OpenLCA. Available online: https://www.openlca.org/the-idea/ (accessed on 26 June 2021).
78. Ntziachristos, L.; Samaras, Z. *EMEP/EEA Emission Inventory Guidebook 2009*; European Environment Agency (EEA): Copenhagen, Denmark, 2009.
79. Jessen, C.; Roder, C.; Villa Lizcano, J.F.; Voolstra, C.R.; Wild, C. In-situ effects of simulated overfishing and eutrophication on benthic coral reef algae growth, succession, and composition in the central Red Sea. *PLoS ONE* **2013**, *8*, e66992. [CrossRef]
80. Selman, M.; Greenhalgh, S. Eutrophication: Sources and Drivers of Nutrient Pollution. WRI Policy Note, Water Quality: Utrophication and Hypoxia. Available online: https://files.wri.org/d8/s3fs-public/pdf/eutrophication_sources_and_drivers.pdf (accessed on 26 June 2021).
81. Hauschild, M.; Potting, J. Spatial Differentiation in Life Cycle Impact Assessment-The EDIP2003 Methodology. Available online: https://lca-center.dk/wp-content/uploads/2015/08/Spatial-differentiation-in-life-cycle-impact-assessment-the-EDIP2003-methodology.pdf (accessed on 26 June 2021).
82. Kim, T.H.; Chae, C.U. Environmental impact analysis of acidification and eutrophication due to emissions from the production of concrete. *Sustainability* **2016**, *8*, 578. [CrossRef]
83. Pulles, T.; Denier van der Gon, H.; Appelman, W.; Verheul, M. Emission factors for heavy metals from diesel and petrol used in European vehicles. *Atmos. Environ.* **2012**, *61*, 641–651. [CrossRef]
84. Fawer, M.; Concannon, M.; Rieber, W. Life cycle inventories for the production of sodium silicates. *Int. J. Life Cycle Assess.* **1999**, *4*, 207. [CrossRef]
85. Koiwanit, J.; Manuilova, A.; Chan, C.; Wilson, M.; Tontiwachwuthikul, P. A comparative study of human health impacts due to heavy metal emissions from a conventional lignite coal-fired electricity generation station, with post-combustion, and oxy-fuel combustion capture technologies. In *Greenhouse Gases: Selected Case Studies*; Manning, A., Ed.; IntechOpen: London, UK, 2016. [CrossRef]
86. Castleden, W.M.; Shearman, D.; Crisp, G.; Finch, P. The mining and burning of coal: Effects on health and the environment. *Med. J. Aust.* **2011**, *195*, 333–335. [CrossRef]
87. Atilgan, B.; Azapagic, A. Life cycle environmental impacts of electricity from fossil fuels in Turkey. *J. Clean. Prod.* **2015**, *106*, 555–564. [CrossRef]
88. Worrell, E.; Price, L.; Martin, N.; Hendriks, C.; Meida, L.O. Carbon dioxide emissions from the global cement industry. *Annu. Rev. Environ. Resour.* **2001**, *26*, 303–329. [CrossRef]
89. Schorcht, F.; Kourti, I.; Scalet, B.M.; Roudier, S.; Sancho, L.D. *Best Available Techniques (BAT) Reference Document for the Production of Cement, Lime and Magnesium Oxide*; European Commission Joint Research Centre Institute for Prospective Technological Studies: Seville, Spain, 2013.
90. Huijbregts, M.A.; Steinmann, Z.J.; Elshout, P.M.; Stam, G.; Verones, F.; Vieira, M.D.M.; Hollander, A.; Zijp, M.; van Zelm, R. *ReCiPe2016. A Harmonized Life Cycle Impact Assessment Method at Midpoint and Endpoint Level. Report I: Characterization*; RIVM Report 2016-0104; National Institute for Human Health and the Environment: Bilthoven, The Netherlands, 2016. Available online: https://www.rivm.nl/bibliotheek/rapporten/2016-0104.pdf (accessed on 15 June 2021).
91. Bosoaga, A.; Masek, O.; Oakey, J.E. CO_2 capture technologies for cement industry. *Energy Procedia* **2009**, *1*, 133–140. [CrossRef]
92. EuroChlor. The European chlor-alkali industry: An Electricity Intensive Sector Exposed to Carbon Leakage. Brussels, Belgium. 2010. Available online: https://www.eurochlor.org/wp-content/uploads/2019/04/3-2-the_european_chlor-alkali_industry_-_an_electricity_intensive_sector_exposed_to_carbon_leakage.pdf (accessed on 26 June 2021).